

# Thermodynamics of CO<sub>2</sub> adsorption on mesoporous materials impregnated with nickel

## *(Termodinâmica da adsorção de CO<sub>2</sub> em materiais mesoporosos impregnados com níquel)*

A. R. do Nascimento<sup>1\*</sup>, G. P. de Figueredo<sup>2,3</sup>, T. R. da Costa<sup>4</sup>, M. A. de F. Melo<sup>1,4</sup>,  
D. M. de A. Melo<sup>2,4</sup>, M. J. B. de Souza<sup>5</sup>

<sup>1</sup>Graduate Program in Chemical Engineering, Chemical Engineering Department, Technology Center;

<sup>2</sup>Graduate Program in Chemistry, Chemistry Department; <sup>4</sup>Graduate Program in Material Science and Engineering, Center of Exact Sciences and Earth, Federal University of Rio Grande do Norte, Lagoa Nova Campus, C.P. 1524, Natal, RN, Brazil 59078-970

<sup>3</sup>Academic Department of Chemistry, Federal Institute of Maranhão, Av Getulio Vargas 4, São Luis, MA, Brazil 65030-005

<sup>5</sup>Graduate Program in Chemical Engineering, Chemical Engineering Department, Center of Exact Sciences and Technology, Federal University of Sergipe, Av. Marechal Rondon s/n, São Cristóvão, SE, Brazil 49100-000  
\*ale3ufs@yahoo.com.br

### Abstract

The adsorption capacity of CO<sub>2</sub> in mesoporous materials with different structures was evaluated. For this purpose, MCM-48 and SBA-15 impregnated with nickel in proportions of 5, 10 and 20 wt% were used. The results showed that impregnation of nickel promoted an increased interaction between CO<sub>2</sub> and the surface of the material. Data were fitted using the Freundlich model. Gibbs free energy and entropy changes of the adsorption system were evaluated. Thermodynamics of adsorption showed that the process is spontaneous. From the Freundlich model, it was concluded that there is a strong interaction of CO<sub>2</sub> with sites of the impregnated materials.

**Keywords:** SBA-15, MCM-48, CO<sub>2</sub> adsorption, Freundlich model.

### Resumo

A capacidade de adsorção de CO<sub>2</sub> em materiais mesoporosos com estruturas diferentes foi avaliada. Para este efeito, MCM-48 e SBA-15 impregnados com níquel em proporções de 5%, 10% e 20% (m/m) foram utilizados. Os resultados mostraram que a impregnação com níquel promoveu um aumento da interação entre o CO<sub>2</sub> e a superfície do material. Os dados foram ajustados utilizando o modelo de Freundlich. As variações de energia livre de Gibbs e entropia do sistema de adsorção foram avaliadas. A termodinâmica de adsorção mostrou que o processo é espontâneo. A partir do modelo de Freundlich concluiu-se que existe uma forte interação do CO<sub>2</sub> com os sítios dos materiais impregnados.

**Palavras-chave:** SBA-15, MCM-48, adsorção de CO<sub>2</sub>, modelo de Freundlich.

## INTRODUCTION

The emission of greenhouse gases such as carbon dioxide has increased considerably in recent years, mainly due to fossil fuel burning for energy generation and for transport. Although the transition to more sustainable energy sources has been an urgent necessity for environmental sustainability, fossil fuels shall remain the dominant energy source. Therefore, reducing CO<sub>2</sub> emission into the atmosphere in addition to its capture and storage is recognized as the main strategies to deal with global warming [1, 2]. Some technologies have been used for CO<sub>2</sub> capture, such as membrane separation, cryogenic methods,

hydrate processes and electrochemical techniques. These alternative technologies have been adapted and developed for the capture of CO<sub>2</sub> in processes such as post-combustion, pre-combustion, and gasification, among others, using different types of materials, i.e. zeolites, activated carbon, pillared clay, metallic oxides or organic metals [1, 3, 4].

There has also been a growing use of molecular sieves based on silica in applications such as separation, adsorption and catalysis [5-7]. Some pure and modified mesoporous materials with amines have been evaluated for CO<sub>2</sub> adsorption [8]. These materials exhibit textural properties, thermal, hydrothermal and mechanical stability suitable for various applications. A chemometric study of the adsorption

of CO<sub>2</sub> on different mesoporous structures of MCM-48 and SBA-15, pure and impregnated with nickel, was reported in [9], by assessing the application of CO<sub>2</sub> adsorbed on dry reforming of methane on supported nickel catalysts. However, there are no studies in literature on evaluating the phenomenological aspects of the thermodynamics in this adsorption process. In the literature, gas adsorption processes on solid materials are made according to temperature variation. In this work, experimental results are presented on the behavior of MCM-48 and SBA-15 adsorbents for both impregnated and not impregnated with nickel for adsorption of CO<sub>2</sub> at a certain pressure range. With these data adjusted to the Freundlich model, changes in Gibbs free energy and entropy of the process according to the pressure were obtained, which are presently not found in the literature.

## EXPERIMENTAL

**Materials:** the materials used in this work were synthesized and characterized in [9] and reported as potential adsorbents for CO<sub>2</sub> capture. As reported [9], the preparation of MCM-48 and SBA-15 mesoporous adsorbents were done through the hydrothermal method, following procedures described in [10, 11] with suitable modifications. The samples were impregnated with nickel by post-synthetic impregnation as well as by contact processes in proportions of 5%, 10% and 20% by weight, using a solution of hexahydrate nickel nitrate dissolved in isopropyl alcohol. After the calcination of samples at 450 °C for 2 h in synthetic air, the nickel nitrate was transformed to nickel oxide [9].

**Adsorption capacity:** the adsorption tests were done by applying the gravimetric method in Rubothermm micro-adsorber equipment. The methodology was performed in three steps: (a) sample activation, (b) determination of thrust effect to correct the values recorded by the balance during the adsorption step, and (c) adsorption of CO<sub>2</sub>, as described in [9, 12]. The adsorption measurement reaches the end when it achieves balance, in other words, without any variation in sample mass. The results from adsorption measurements were presented in graphs from the relation between absorbed mass and adsorbent mass as a function of pressure (isotherm). The parameters used to perform the analysis were: temperature (298 K); absolute pressure (100 to 4000 kPa); sample activation temperature (398 K); sample activation pressure (vacuum); activation time (2 h); and adsorbate (CO<sub>2</sub>). The obtained data were adjusted through the Freundlich model and the measured thermodynamic parameters were Gibbs free energy and

entropy of adsorption system.

**Thermodynamic models:** Freundlich's adsorption of isotherms was used to describe heterogeneous adsorbent data; this model suggests that the energy of adsorption decreases logarithmically as the surface is covered by solute. This makes it different from the Langmuir equation. The Freundlich model accepts adsorption in layers, where the capacity of adsorption Q is given by [13]:

$$Q = K_F C_e^{1/n} \quad (A)$$

where,  $K_F$  is the Freundlich constant related to adsorption capacity,  $n$  is the empirical parameter which is related to adsorption intensity, and  $C_e$  is the solute balance concentration in solution (mg.L<sup>-1</sup>). The values of  $n$  in the range 1 to 10 indicate favorable adsorption. The Freundlich linearized equation is given by:

$$\ln Q = \ln K_F + \frac{1}{n} \ln C \quad (B)$$

In the plot of  $\ln(Q)$  as a function of  $\ln(C)$ , the intercept is  $\ln(K_F)$  and the slope is  $1/n$ . The deviation of a real gas from the ideal gas behavior can be shown by an empirical factor inserted in an ideal gas equation, called compressibility Z factor (as a function of temperature, T, and pressure, P). This factor shows the following conditions: for a perfect gas,  $Z=1$  and, at any condition, the deviation of Z from 1 is a measure of the removal of the gas related to an ideal behavior. At very low pressure, all gases have  $Z \approx 1$  and they behave almost perfect. At high pressure, all gases have  $Z > 1$ , indicating a molar volume of the gas higher than a perfect gas; the repulsive forces are dominant. At intermediate pressure, most of gases have  $Z < 1$ , indicating that attractive forces are reducing the molar volume of the gas compared to a perfect gas [14]. For the thermodynamic parameters in studies of adsorption, the compressibility Z factor in each operating pressure was investigated. The Z data was obtained by interpolation of the values presented in Table I of carbon dioxide, at some temperature range, found in [15]. With the obtained Z data, the volume, V, of the adsorption process was calculated for each pressure at a constant temperature by:

$$V = \frac{n_i \text{ mol}}{P_i} ZRT \quad (C)$$

With obtained volume data, the changes in Gibbs free energy (Equation D) and entropy (Equation E) were calculated. Gibbs free energy change is a thermodynamic function which states the spontaneous transformation in terms of the system's state functions [14].

Table I - Compressibility Z factor of carbon dioxide at 298 K.

[Tabela I - Fator de compressibilidade Z do dióxido de carbono em 298 K.]

Pressure (kPa)	100	300	500	1000	2000	3000	4000
Z	0.99485	0.983448	0.97315	0.94505	0.883545	0.818218	0.75205

$$G(P_i) = G(P_i) + V \int_{P_i}^{P_f} dP \quad (D)$$

$$\Delta S = - \frac{\Delta G}{T} \quad (E)$$

## RESULTS AND DISCUSSION

Figs. 1a and 1b show the results from CO<sub>2</sub> adsorption tests for the investigated adsorbents, at pressures of 100 and 4000 kPa, respectively. It can be observed in Fig. 1a that impregnation with 5 and 10 wt% of nickel for the MCM-48 adsorbent provided a slight increase in CO<sub>2</sub> adsorption capacity in low pressure, possibly due to contribution from an interaction between nickel oxide and CO<sub>2</sub>. For SBA-15, it was observed that an impregnation with different nickel contents decreased the CO<sub>2</sub> adsorption capacity, showing that nickel oxide did not contribute positively in this case to

the adsorbed amount. On the other hand, the data presented in Fig. 1b reveal that the quantity of CO<sub>2</sub> adsorbed by the materials was higher than the ones presented when done at 100 kPa. SBA-15 presented a similar behavior to the one submitted at 100 kPa, with a reduction in the quantity adsorbed as the impregnated nickel content increased. On the other hand, MCM-48 presented a prominent change in behavior, especially for the adsorbed quantity from impregnated samples. This may be a consequence of different textural characteristics from MCM-48 and SBA-15, as reported in [9]. Therefore, it can be concluded that different mesoporous structures show distinct behavior when submitted to different operating pressures of CO<sub>2</sub> adsorption [9]. Comparing the obtained results of CO<sub>2</sub> adsorption with literature data, it was observed that SBA-15 approached the adsorptive capacity of the activated carbon at low pressure conditions, as shown in Table II. The adsorption capacity

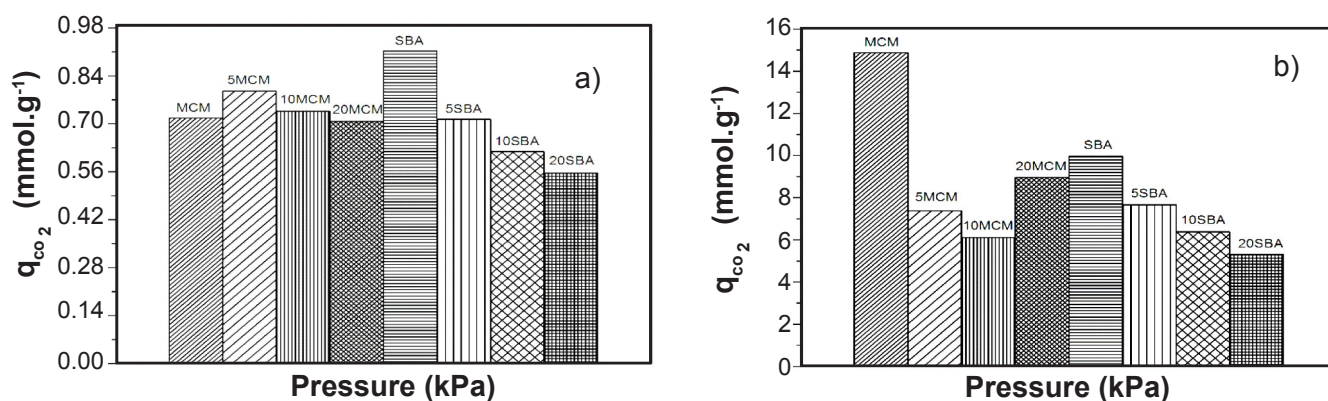


Figure 1: Quantity of CO<sub>2</sub> adsorbed at 100 kPa (a) and 4000 kPa (b) for the samples MCM-48 (MCM), 5Ni-MCM-48 (5MCM), 10Ni-MCM-48 (10MCM), 20Ni-MCM-48 (20MCM), SBA-15 (SBA), 5Ni-SBA-15 (5SBA), 10Ni-SBA-15 (10SBA), and 20Ni-SBA-15 (20SBA). [Figura 1: Quantidade de CO<sub>2</sub> adsorvida a 100 kPa (a) e 4000 kPa (b) para as amostras de MCM-48 (MCM), 5Ni-MCM-48 (5MCM), 10Ni-MCM-48 (10MCM), 20Ni-MCM-48 (20MCM), SBA-15 (SBA), 5Ni-SBA-15 (5SBA), 10Ni-SBA-15 (10SBA) e 20Ni-SBA-15 (20SBA).]

Table II - Adsorption data at determined pressure range to different material found in literature. [Tabela II - Dados de adsorção em uma determinada faixa de pressão para diferentes materiais encontrados na literatura.]

Material	Pressure range (kPa)	CO <sub>2</sub> adsorption capacity (mmol.g <sup>-1</sup> )	Reference
Zeolite LiX	100-1000	3.2-5.4	[16]
Activated coal	100-1000	1.1-6.2	[16]
Tripe-MCM-41	100-2500	2.42-6.50	[1]
PEI-50/SBA-15	5000	2	[17]
APTS-MCM-48 (RHA)	100	0.64	[18]
MCM-48 (RHA)	100	0.033	[18]
Mg-SBA-15	100	0.493	[19]
MCM-48	100-1000	0.72-4.75	This work
MCM-48	2000-4000	7.87-15.83	This work
SBA-15	100-1000	0.91-4.19	This work
SBA-15	2000-4000	6.26-8.36	This work

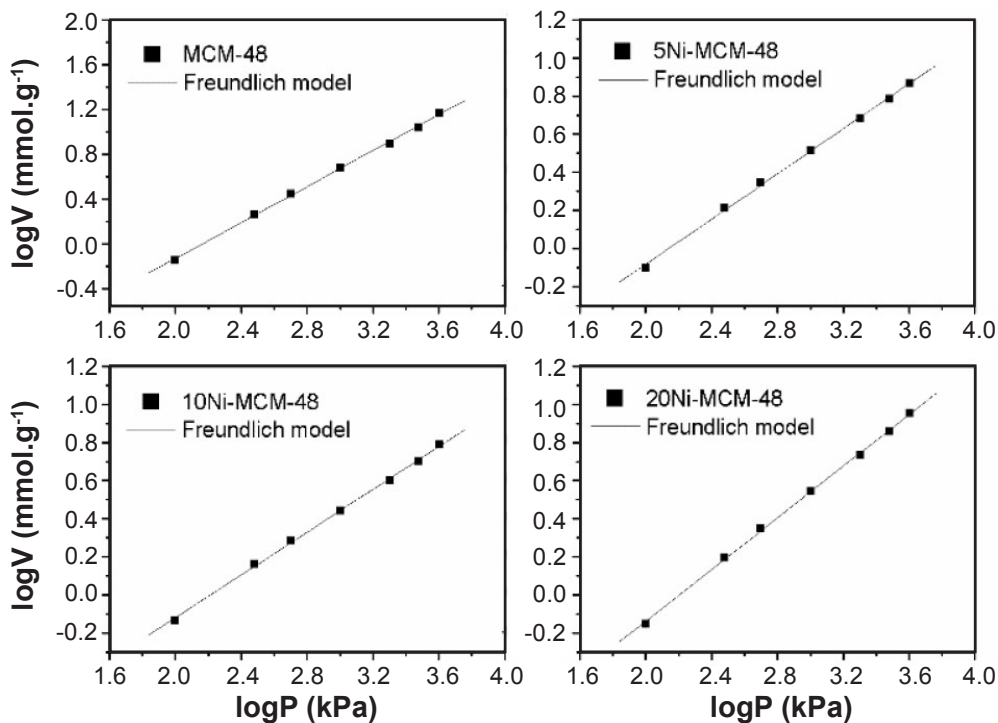


Figure 2: CO<sub>2</sub> adsorption data fitting to Freundlich model for the samples of MCM-48 series.

[Figura 2: Ajustes de adsorção do CO<sub>2</sub> para o modelo de Freundlich para as amostras da série MCM-48.]

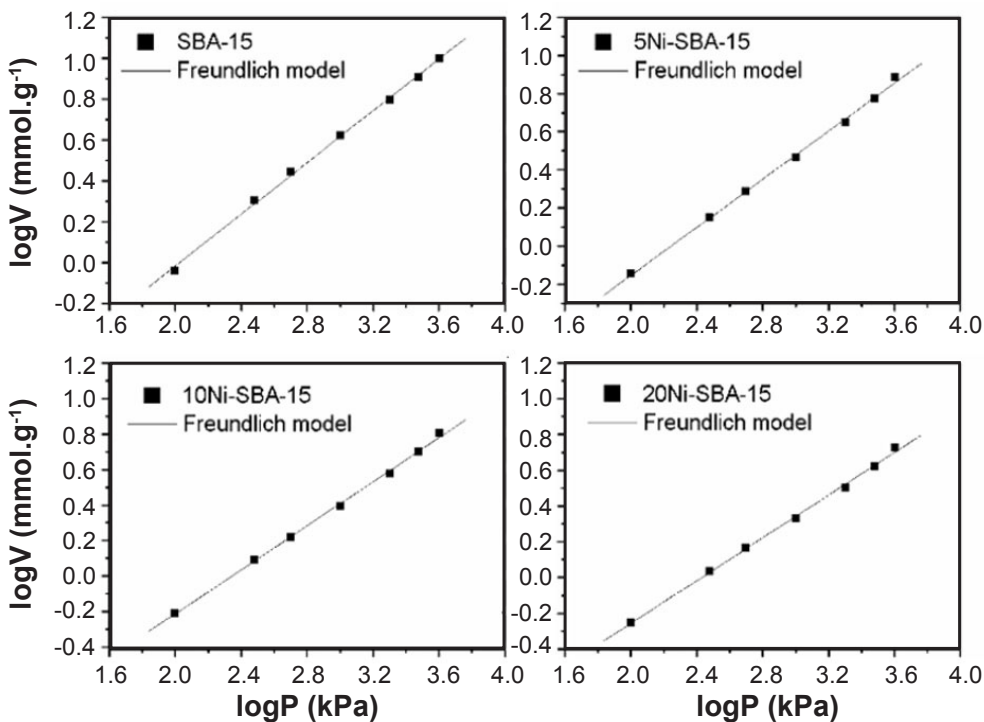


Figure 3: CO<sub>2</sub> adsorption data fitting to Freundlich model for the samples SBA-15 series.

[Figura 3: Ajustes de adsorção do CO<sub>2</sub> para o modelo de Freundlich para as amostras da série SBA-15.]

of the material increased with increasing pressure, getting close (in some cases even higher) values than the modified adsorbent and those reported in literature.

The obtained adsorption data were adjusted to the Freundlich model and are shown in Figs. 2 and 3 for the samples MCM-48, 5Ni-MCM-48, 10Ni-MCM-48, 20Ni-

MCM-48 and SBA-15, 5Ni-SBA-15, 10Ni-SBA-15, 20Ni-SBA-15, respectively. Table III describes the data obtained from the Freundlich model adjusted to the investigated samples. In Figs. 2 and 3, it is observed that the obtained data of the CO<sub>2</sub> adsorption were properly adapted to the Freundlich model, showing values of linear correlation R<sup>2</sup>

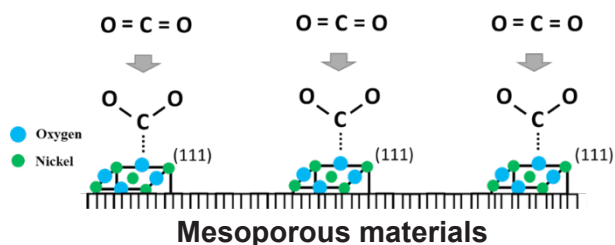


Figure 4: Proposed mechanism to describe the adsorption of CO<sub>2</sub> on the NiO sites.

[Figura 4: Mecanismo proposto para descrever a adsorção do CO<sub>2</sub> sobre os sítios de NiO.]

close to 1. According to Table III, it is noticed that for MCM-48 samples the constant  $n$  in relation to the affinity of CO<sub>2</sub> adsorption to material increased with nickel impregnation, while constant  $k$ , in relation to adsorptive capacity of MCM-48, also increased, except for 20Ni-MCM-48. However, a reduction in quantity of CO<sub>2</sub> adsorbed for impregnated samples was observed, possibly due to a blockade occurring at the entrance of the porous channels of the adsorbents in the impregnation step, hindering the CO<sub>2</sub> access into the adsorption site. Different behavior was observed for SBA-15 samples. The increased nickel content increased the affinity of the CO<sub>2</sub> with the adsorbent surface; however, the constant  $k$  decreased with impregnation, confirming the obtained data of the adsorption, in which a reduction of the gas adsorptive capacity to modified materials was observed. In this case, it can be previously concluded that CO<sub>2</sub> strongly interacts with nickel oxide in site, preventing that new molecules may adsorb, thus reflecting a lesser amount of CO<sub>2</sub> adsorbed when nickel content is increased. All investigated material showed values of  $n > 0$ , showing that the CO<sub>2</sub> adsorption conditions were favorable. The proposed mechanism to describe the adsorption of CO<sub>2</sub> on the NiO sites is described in Fig. 4; it can be observed that the adsorption occurs in the planes (111) because they are considered the most active due to their lower coordination number [20].

Table III - Fitting parameters to Freundlich model for CO<sub>2</sub> adsorption for investigated samples.

[Tabela III - Parâmetros de ajuste para o modelo de Freundlich para adsorção de CO<sub>2</sub> das amostras investigadas.]

Sample	R <sup>2</sup>	k	n
MCM-48	0.9994	0.018	1.25
5Ni-MCM-48	0.9994	0.054	1.69
10Ni-MCM-48	0.9994	0.057	1.78
20Ni-MCM-48	0.9997	0.032	1.47
SBA-15	0.9991	0.052	1.58
5Ni-SBA-15	0.9991	0.038	1.58
10Ni-SBA-15	0.9992	0.035	1.61
20Ni-SBA-15	0.9992	0.035	1.67

Using obtained data from Gibbs free energy variation calculations as a function of pressure and the use of the compressibility factor for correction of deviant behavior of a real gas, the changes in energy and entropy of the adsorption system were obtained for all samples. The calculated values were very similar, therefore, only one MCM-48 and one SBA-15 samples were used. Fig. 5 shows the data obtained for the energy and entropy changes of the adsorption system, and are represented by overlapping sample curves. The values showed that CO<sub>2</sub> adsorption process occurred in a spontaneous way, as the change in Gibbs free energy was negative. For pressure below 1000 kPa, it was observed that the adsorption process was more spontaneous, and for pressure above 1000 kPa, Gibbs free energy change was practically constant, only observing subtle variations. This was in agreement with the change in entropy, since a decrease in entropy change occurred at pressures below 1000 kPa, confirming that adsorption process occurred in a spontaneous way and approached the balance of pressure above 1000 kPa [14]. With decreasing entropy change, the CO<sub>2</sub> adsorbed molecules lose their

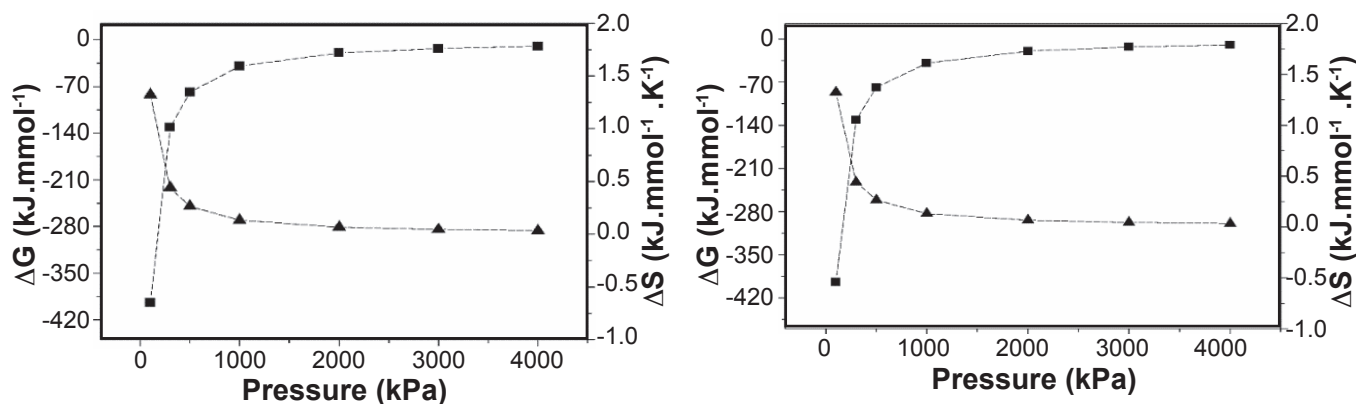


Figure 5: Changes in Gibbs free energy,  $\Delta G$  (□), and entropy,  $\Delta S$  (Δ), of CO<sub>2</sub> adsorption in pressure range from 100 to 4000 kPa, for samples of: (a) MCM-48 series; and (b) SBA-15 series.

[Figura 5: Variação de energia livre de Gibbs,  $\Delta G$  (□), e entropia,  $\Delta S$  (Δ), na adsorção de CO<sub>2</sub> na faixa de 100 a 4000 kPa para as amostras da: (a) série MCM-48; e (b) série SBA-15.]

degree of freedom and decrease system disorder [14]. For pressure above 1000 kPa, entropy change was close to zero, and it can be related to real gas behavior, as repulsive forces are significant when molecules are in contact. Also, because they are short-range interactions, the repulsions become significant when the average separation among molecules is small. This is the case in high pressure, when a high number of molecules use a small volume in space. The attractive intermolecular forces have a relatively large range interaction and they are effective in distances of various molecular diameters [14].

## CONCLUSIONS

The obtained data from adsorption tests fitted to the Freundlich model proved to be a favorable process. From the Freundlich model, it was concluded that there is affinity with adsorbent CO<sub>2</sub>, therefore, the adsorption capacity was possibly compromised due to blockade at the entrance of the porous channels from adsorbents, as well as a strong interaction of CO<sub>2</sub> with nickel oxide site. Thermodynamics of adsorption showed that the process was spontaneous because the change in Gibbs free energy was negative, as well as the change in entropy which decreased as the pressure increased, approaching to zero. MCM-48 and SBA-15 modified with nickel showed a strong interaction with CO<sub>2</sub> molecules, indicating that these materials show potential use in industrial process where adsorbents in strong active sites are demanded.

## ACKNOWLEDGEMENTS

The authors acknowledge LCR/LABTAM/NUPPRAR (Catalysis and Refine Laboratory and Environmental Technologies Laboratory from Center of Primary Processing and Reuse of Produced Water and Waste) at Federal University of Rio Grande do Norte - UFRN and CAPES-Brazil (Improving Coordination of Superior Academic Level People) for the support of this research.

## REFERENCES

- [1] Y. Belmabkhout, R. Serna-Guerrero, A. Sayari, *Adsorption* **17** (2011) 395.
  - [2] S. Loganathan, M. Tikmani, S. Edubilli, A. Mishra, A.K. Ghoshal, *Chem. Eng. J.* **256** (2014) 1.
  - [3] Y. Belmabkhout, A. Sayari, *Adsorption* **15** (2009) 318.
  - [4] J.A.B.L.R. Alves, G.P. Figueredo, R.L.B.A. Medeiros, T.R. Costa, D.M.A. Melo, M.A.F. Melo, *Cerâmica* **62** (2016) 77.
  - [5] C.T. Kresge, M.E. Leonowicz, W.J. Roth, J.C. Vartuli, J.S. Beck, *Nature* **359** (1992) 710.
  - [6] A. Tadjarodi, V. Jalalat, R. Zare-Dorabei, *Mater. Res. Bull.* **61** (2014) 113.
  - [7] R. Zare-Dorabei, V. Jalalat, A. Tadjarodi, *New J. Chem.* **40** (2016) 5128.
  - [8] T.G. Oliveira, S.W.M. Machado, S.C.G. Santos, M.J.B. Souza, A.M.G. Pedrosa, *Quim. Nova* **37** (2014) 610.
  - [9] A.R. Nascimento, G.P. Figueredo, G. Rodrigues, M.A.F. Melo, M.J.B. Souza, D.M.A. Melo, *Cerâmica* **60** (2014) 482.
  - [10] A. Doyle, B.K. Hodnett, *Microporous Mesoporous Mater.* **63** (2003) 53.
  - [11] S. Brunauer, P.H. Emmett, E. Teller, *J. Am. Chem. Soc.* **60** (1938) 309.
  - [12] C.C. Costa, D.M.A. Melo, M.A.F. Melo, M.E. Mendoza, J.C. Nascimento, J.M. Andrade, J.M.F. Barros, *J. Porous Mater.* **21** (2014) 1069.
  - [13] R. Ciola, *Fundamentos da catálise*, Ed. Moderna, Ed. Univ. S. Paulo, S. Paulo (1981).
  - [14] P.W. Atkins, J. Paula, *Físico-química*, 9<sup>a</sup> ed., LCT, Rio de Janeiro, Vol. 1 (2013).
  - [15] R.H. Perry, C.H. Chilton, *Chemical engineers handbook*, Ed. Guanabara Dois, Rio de Janeiro (1980).
  - [16] Y. Park, D-K. Moon, Y-H. Kim, H. Ahn, C-H Lee, *Adsorption* **20** (2014) 631.
  - [17] X. Wang, X. Ma, C. Song, D.R. Locke, S. Siefert, R.E. Winans, J. Möllmer, M. Lange, A. Möller, R. Gläser, *Microporous Mesoporous Mater.* **169** (2013) 103.
  - [18] H.T. Jang, Y.K. Park, Y.S. Ko, J.Y. Lee, B. Margandan, *Int. J. Greenh. Gas Control* **3** (2009) 545.
  - [19] A. Zupal, J. Pastva, J. Cejka, *Microporous Mesoporous Mater.* **167** (2013) 44.
  - [20] T. Matsumoto, J. Kubota, J.N. Kondo, C. Hirose, K. Domen, *Langmuir* **15** (1999) 2158.
- (*Rec. 06/08/2016, Rev. 08/12/2016, Ac. 27/02/2017*)